Materials Science and Engineering B 264 (2021) 114951

Contents lists available at ScienceDirect

Materials Science & Engineering B

journal homepage: www.elsevier.com/locate/mseb

# A novel electrochemical sensor modified with green gold sononanoparticles and carbon black nanocomposite for bisphenol A detection

Siwar Jebril [a,b], Laura Cubillana-Aguilera [c], José María Palacios-Santander [c,*], Chérif Dridi [a,*]

[a] NANOMISENE Laboratory, LR16CRMN01, Centre for Research on Microelectronics and Nanotechnology (CRMN) of Technopole of Sousse, B. P334, 4054 Sahloul Sousse, Tunisia

[b] University of Sousse, High School of Sciences and Technology of Hammam, Sousse, Tunisia

[c] Institute of Research on Electron Microscopy and Materials (IMEYMAT), Department of Analytical Chemistry, Faculty of Sciences, Campus de Excelencia Internacional del Mar (CEIMAR), University of Cadiz, Campus Universitario de Puerto Real, Polígono del Río San Pedro S/N, 11510 Puerto Real, Cádiz, Spain

ARTICLE INFO

*Keywords:*
Gold sononanoparticles
Bisphenol A
Carbon black
Green synthesis
Electrochemical sensor

ABSTRACT

Herein, we report an eco-friendly electrochemical bisphenol A (BPA) sensor based on carbon black (CB) and gold sononanoparticles (AuSNPs) nanocomposite-modified Sonogel-Carbon electrode (SNGCE). The AuSNPs were synthesized by a novel green approach employing olive leaves extract and assisted by high energy ultrasound. The AuSNPs was characterized by UV–Vis, FTIR, SEM and STEM. The formation of AuSNPs was confirmed by UV–Vis, which showed an absorption peak at 532 nm. The FTIR analysis identified the bioactive molecules present in the olive leaves which were responsible for the bioreduction and capping of the nanoparticles. STEM results evidenced the polymorphic nature of the biosynthesized AuSNPs and the average size of about $14 \pm 1$, $39 \pm 5$ and $20 \pm 1$ nm, respectively for spherical, triangular and hexagonal nanoparticles. The CB/AuSNPs/SNGCE sensor for BPA determination showed higher electroactivity, with the highest sensitivity, and a rather low limit of detection (LOD, $n = 3$) of 60 nM at the BPA concentration range of 0.5–15 μM, thanks to the synergic combination of green AuSNPs and CB as cost-effective nanomaterials. Furthermore, our developed sensor showed an excellent selectivity towards different interferents. Besides, the analytical sensor was successfully applied for the determination of BPA in tap and mineral water samples.

## 1. Introduction

Bisphenol A (BPA) is a significant plastic product in our life. It is mostly transferred into foods and drinks from plastic products, including water bottles, lining of food cans, and dental fillings [1–3]. It is known that BPA is considered as an endocrine-disrupting compound, related to various kinds of health concerns, such as the development of cancers, and reproduction problems [4,5]. Thus, as a matter of public health, the development of a reliable analytical approach for BPA determination supposes an urgent issue.

Various analytical approaches have been established for BPA determination, including chromatography [6,7], electrophoresis [8,9], and enzyme-linked immunosorbent assay (ELISA) [10,11]. However, all these techniques are expensive, hard to control and request a longer period. By opposite, due to simple operation, low cost, high sensitivity, rapidity, and selectivity, the electrochemical methods are recently considered to be one of the most important and promising techniques for the determination of BPA, essentially when the modification of the surface of the electrode is employed to enhance the sensitivity of sensors [12,13].

Carbon black (CB) is a cost-effective nanomaterial characterized by its significantly widespread availability and high surface area to volume ratio [14–16]. It has opened up novel outlooks for the development of low-cost electrochemical sensors with higher electroanalytical performances. Furthermore, apart from the direct use of CB alone in modified working electrodes, it can also be utilized as a support for the elaboration of many other nanomaterials [15,17], leading to different combinations of nanostructured materials that enhance quality analytical parameters of the electrochemical devices, such as higher sensitivity, lower limits of detection and quantification, better stability, reproducibility and repeatability. Some electrode configurations involving different nanomaterials that have been used in the modification of the working electrodes for BPA detection are: multi-walled carbon nanotubes/silica@gold (MWCNT/$SiO_2$@Au) [18], porous graphene

* Corresponding authors.
*E-mail addresses:* josem.palacios@uca.es (J.M. Palacios-Santander), cherif.dridi@crmn.rnrt.tn (C. Dridi).

https://doi.org/10.1016/j.mseb.2020.114951
Received 26 June 2020; Received in revised form 3 November 2020; Accepted 15 November 2020
Available online 1 December 2020

functionalized black phosphorus (PG-BP) [19], nickel nanoparticles/nitrogen-doped carbon nanosheet/chitosan (NiNP/NCN/CS) [13], and carbon black-functionalized multi-walled carbon nanotubes (CB/f-MWCNTs) [20], among others.

Gold nanoparticles (AuNPs) attract much attention due to their specific characteristics, such as excellent conductivity, large surface to volume ratio, good biological compatibility, and high electrocatalytic properties. Besides, this type of nanomaterials has a great potential in the preparation of electrochemical (bio)sensors [21–23]. Various works have used AuNPs for electrode modification in the determination of BPA [3,24,25]. However, the use of physical and chemical procedures for synthesizing AuNPs prompts the utilization of toxic chemical materials, promoting unsuitable effects at nanoscale properties [26]. To overcome these physical and chemical hazards, green synthesis routes have been established to reduce the possible risks. The green methods can be characterized by their easiness of nanoparticles production, cost-effectiveness and eco-friendliness [27–29].

Here, we developed a novel eco-friendly electrochemical BPA sensor based on cost-effective nanomaterials such as CB and green AuSNPs nanocomposite, as well as the also economic and environmentally friendly Sonogel-Carbon (SNGC) electrode as transducer. The green AuSNPs were synthesized by a biological, simple, and faster method from olive leaves extract, which was used as capping and reducing agents assisted by high energy ultrasound. Hence, the novelty of this work relies mainly on the green methodology employed for synthesizing both the receptor/sensitive part (AuSNPs) and the transducer part (SNGC material) of the sensor; moreover and up to the extent of our knowledge, the AuSNPs has been synthesized for the first time from olive leaves extract and using the ultrasound technology. Besides, various techniques were used to characterize these AuSNPs for explaining their morphological, optical, structural and textural properties. Furthermore, the fabricated sensor was constructed to show high sensitivity and low limit of detection (LOD) at the nanomolar level (one of the lowest found in literature for similar devices as far as we know). Thus, the CB/AuSNPs/SNGCE sensor achieved desirable BPA sensing ability with excellent sensitivity and stability. Thus, it can be considered as a very promising sensor for sustainable applications.

## 2. Experimental

### 2.1. Reagents and equipment

Carbon black (CB) (Monarch 570) was obtained from Cabot Corporation through Delta Tecnic, S.A., Spain. Potassium tetrachloroaurate (III) ($KAuCl_4$, 99.99%), dimethylformamide (DMF), bentonite, bisphenol A (BPA), hydrochloric acid and sodium hydroxide were purchased from Sigma-Aldrich, Germany. Dipotassium phosphate ($K_2HPO_4$) was obtained from Panreac, Spain, and monopotassium phosphate ($KH_2PO_4$, >99.5%) was purchased from Merck, Germany, and used to prepare Phosphate Buffer Solution (PBS). Methyltrimethoxysilane (MTMOS, 98%) was also purchased from Merck (Darmstad, Germany). Nanopure (18 MΩ·cm) water from a Millipore Milli-Q system (Bedford, MA) was utilized to prepare the solutions.

### 2.2. Instrumentation

AuSNPs and SNGC materials were synthesized using a high energy ultrasound generator, SONICATOR 3000 from MISONIX Inc. (Farmingdale, NY, USA). Olive leaves extract was prepared by a high energy SONOPLUS HD2200 Ultrasonic Homogenizer from BANDELIN (Berlin, Germany). Biosynthesized AuSNPs were centrifuged with a BIOCEN 22 R centrifuge, from ORTOALRESA (Ortoalresa - Álvarez Redondo, S.A, Daganzo de Arriba, Madrid, Spain). The synthesis of AuSNPs was confirmed using a UV–Visible spectrophotometer (JASCO, Maryland, USA) in the range of 400–700 nm, using a 2 mL cuvette and developing the analysis at room temperature. To obtain the functional groups present in the olive leaves which were responsible for the synthesis and stabilization of the NPs, a Fourier transform infrared (FTIR) spectrophotometer (Shimadzu Corporation, Kyoto, Japan) was employed in the range of 4000–400 $cm^{-1}$. To obtain the FTIR spectra, a freshly synthesized AuSNPs colloidal solution was used directly and the measurement performed in the attenuated total reflection (ATR) mode. The size and morphology of AuSNPs were obtained by a scanning electron microscopy (SEM-FEI Nova NANOSEM 450, USA) at 5 kV. The same equipment was used as well for measuring the samples in the scanning/transmission (STEM) mode with a resolution of 1 nm. Furthermore, in this state, the images were taken at 30 kV (a copper-carbon grid was employed as sample-holder). To obtain the SEM and STEM micrographs, an optimized amount of AuSNPs and CB was dropped on the surface of SNGCEs, and dried at room temperature in darkness. Then, for microscopy study we used one of the electrodes which had not been used in any electrochemical measurement, while the other electrode had been used at least 60 times for the electrochemical determination of BPA. All electrochemical measurements were carried out by an Autolab 302N potentiostat/galvanostat (Ecochemie, The Netherlands) connected with a PC running the software GPES. A three-electrode system was employed: a SNGCE as the working electrode, with an inner diameter of 1.15 mm; a platinum rod as the counter electrode; and Ag/AgCl (3 M) as the reference electrode.

### 2.3. Solutions

Carbon black solution was obtained by sonication of 10 mL of a mixture of nanopure water/DMF (1:1) and 10 mg of CB for 1 h. Stock solution ($10^{-3}$ M) of BPA was dissolved in methanol and diluted using PBS to obtain different concentrations. Phenol, hydroquinone, magnesium ($Mg^{2+}$), calcium ($Ca^{2+}$) and copper ($Cu^{2+}$) salts were diluted using PBS. As real samples, two water samples were employed: tap water obtained directly from the laboratory in Puerto Real city (Spain), and mineral water obtained from a local market.

### 2.4. Preparation of olive leaves extract and synthesis of AuSNPs

The preparation process was adapted from [30]. An amount of 2 g of washed olive leaves was cut and mixed in 10 mL of water; then, sonicated for 10 min using a high energy ultrasound. After that, the aqueous extract was filtered; then, add with stirring 20 mg of bentonite. This obtained solution was refrigerated (24 h) and filtered to separate proteins. 1.25 mL of $KAuCl_4$ (1.5 mM) solution was put in a glass vessel. Later, a high energy ultrasound probe was put into the solution. After 1 min, 160 μL of olive leaves extract were added with a micropipette to the glass vessel. Finally, after only 4.5 min of sonication, the solution changed into red wine color (Scheme 1) [30], indicating the reduction of AuSNPs. Once AuSNPs were synthesized, the solution was centrifuged for 3 min at 3000 rpm.

### 2.5. Preparation of CB/AuSNPs/SNGCE

The Sonogel-Carbon electrodes (SNGCE) were fabricated by following the protocol described previously [31,32]. Afterwards, the surface of the bare SNGCEs was polished using P#1200 emery paper (Struers, Germany) to eliminate any extra material, washed with nanopure water and dried before modification. The AuSNPs/SNGCE was prepared by casting 4 μL of AuSNPs, then was dispersed onto the clean surface of SNGCE and left to dry. To improve the performance of our sensor, the CB amount was optimized. The CB/AuSNPs/SNGCE sensor was fabricated by depositing 0.5, 1 and 2 μL of CB solution on the surface of the prepared AuSNPs/SNGCE; afterwards, drying step was done in darkness.

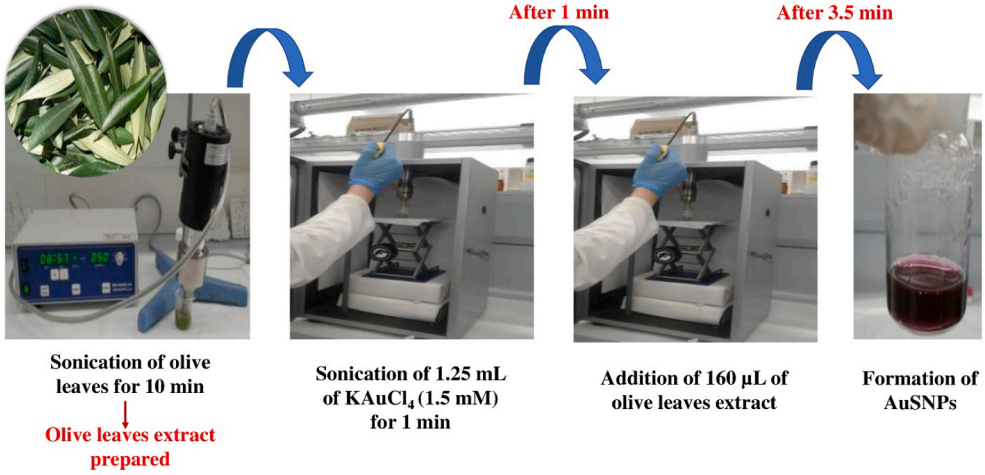


**Scheme 1.** Synthetic route for the biosynthesis of AuSNPs using olive leaves extract as reducing/capping agent and high energy ultrasound to promote the synthesis.

### 2.6. Electrochemical measurements

The electrochemical determination of BPA, under the optimized experimental conditions with the CB/AuSNPs/SNGCE sensor, was performed by successive additions of BPA from the stock solution to obtain different concentrations of BPA within the range of 0.5–15 µM, in an electrochemical cell containing 0.1 M phosphate buffer solution (pH 7). Differential pulse voltammetry (DPV) was used as electroanalytical technique in the range of potential from 0.2 to 0.9 V, at a pulse time of 100 ms, a scan rate of 60 mV·s$^{-1}$, and a pulse amplitude of 100 mV.

## 3. Results and discussion

### 3.1. Characterizations of the biosynthesized AuSNPs

#### 3.1.1. UV–Visible spectroscopy

Gold sononanoparticles were synthesized using olive leaves aqueous extract, in which plant molecules were utilized as reducing and stabilizing agents through a high energy ultrasound-based sonocatalysis process. After 3.5 min, the addition of leaves extract to the $KAuCl_4$ solution makes a change in the mixture color, from yellow to a red color, showing the synthesis of AuSNPs (see Fig. 1.(a)). The active molecules existing in the leaves extract reduces the $Au^{3+}$ ions to Au atoms. Then, atoms form clusters and these generate the nanoparticles that will be stabilized by the biomolecules present in the solution. Fig. 1.(b) illustrate the UV–Visible spectrum of synthesized AuSNPs; showing that the surface plasmon resonance band corresponding to the AuSNPs indicated a maximum peak at 532 nm, as expected according to the literature [33,34].

#### 3.1.2. FTIR analysis

FTIR spectrum of the olive leaves extract and the synthesized AuSNPs are shown in Fig. 2. FTIR analysis was utilized to obtain the main groups of the biomolecules existing in the olive leaves responsible for the synthesis of AuSNPs. Fig. 2.(a) shows that the band at 3357 cm$^{-1}$ corresponds to carbonyl O—H groups, related to oleuropein, present in the olive leaves [35]. Otherwise, the peak at 2102 cm$^{-1}$ can be related to alkyne groups. The strong band at 1638 cm$^{-1}$ corresponds to amide I emerging due to carbonyl spread in proteins. Besides, the peak at 650 cm$^{-1}$ is referred to C—H out of plane bending vibrations of replaced ethylene systems —CH=CH [36]. In the case of AuSNPs, a shift in the absorbance peak at 3357 cm$^{-1}$ to 3349 cm$^{-1}$ might indicate the binding of gold atoms with hydroxyl groups of the leaves extract [35]. Besides, the presence of the band due to amide I indicate the possibility that

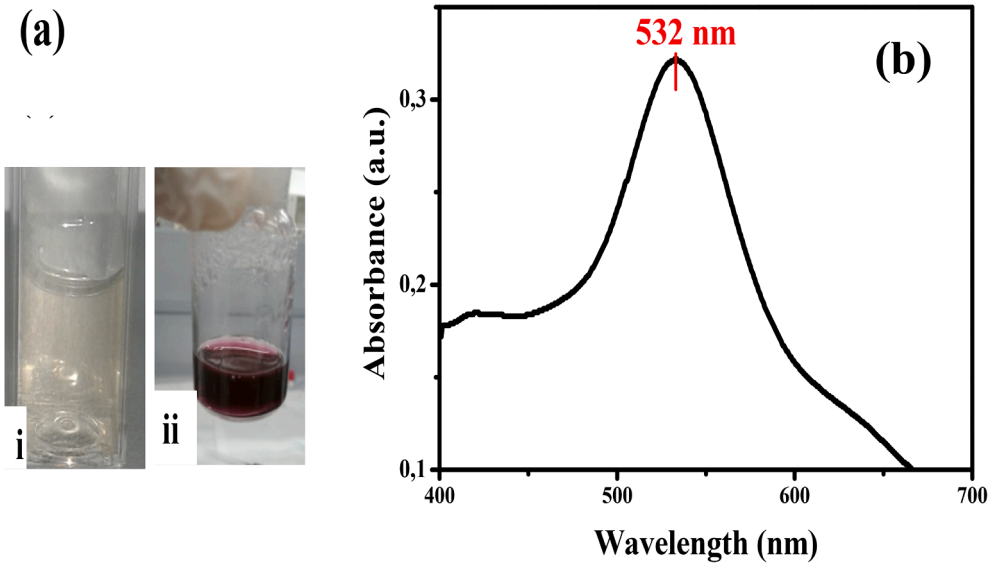


**Fig. 1.** (a) Olive leaves extract (i) and AuSNPs colloid (ii) solutions; (b) UV–Visible spectrum of biosynthesized AuSNPs after the synthesis with olive leaves extract.

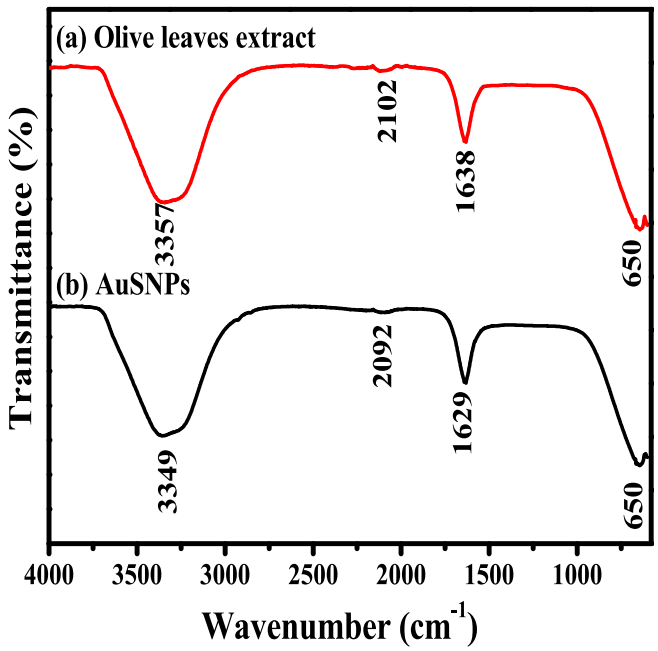


**Fig. 2.** FTIR spectra of (a) olive leaves extract and (b) synthesized AuSNPs.

AuSNPs are bound to proteins existing in the extract of the olive leaves, as well as the hydroxyl groups, that are responsible for the bioreduction and stabilization of the synthesized AuSNPs. The proposed mechanism for the synthesis of green AuSNPs using olive leaves extract is shown in Scheme 2.

### 3.1.3. STEM studies

The size and morphology of the biosynthesized AuSNPs were obtained from STEM micrographs at high magnifications (120,000× and 240,000×) (Fig. 3). STEM results showed that NPs have various morphologies, such as spherical, triangular, hexagonal, and rod-shaped NPs. Moreover, as it is well known, the electrocatalytic activity of NPs strongly belongs to their morphology and size [37,38]. Besides, various works indicate that the electrocatalytic activity should be preferred when the NPs are characterized by different facets and/or have more edges [39]. Thus, the attendance of polygonal NPs could be an advantage for sensing purposes rather than spherical ones. Here, the spherical NPs showed rather homogeneous distribution, such that the average size is approximately 14 ± 1 nm and with a percentage of around 15% of NPs. Regarding the triangular NPs, they were bigger in size at about 39 ± 5 nm and displayed a more heterogeneous distribution with a low percentage of about 10% of NPs. Finally, the hexagonal NPs also showed more homogeneous distribution, like spherical ones but a bit much bigger, with an average size of 20 ± 1 nm and with a high percentage exceeding 72% of NPs. Also, there is a low and negligible percentage of NPs belonging to other less abundant morphologies.

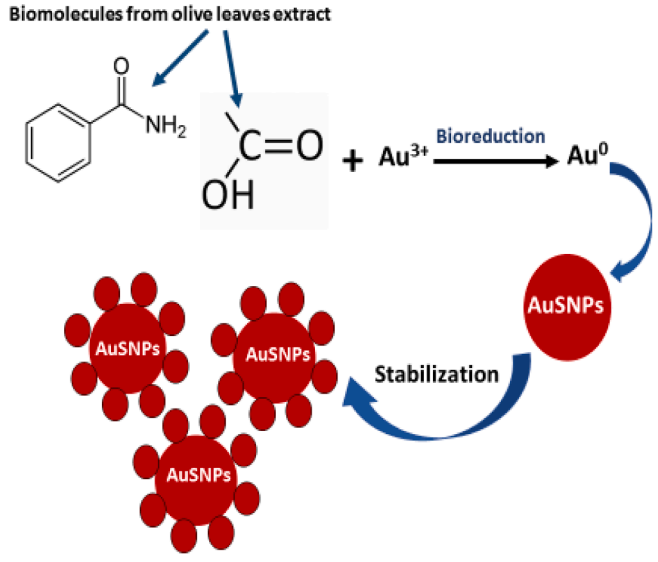


**Scheme 2.** Proposed mechanism for the biosynthesis of AuSNPs using olive leaves extract.

## 3.2. Electrochemical characterization

### 3.2.1. Electrochemical characterization of the modified SNGCE

The electrochemical properties of the modified electrodes were characterized by DPV in the presence of BPA. Fig. 4 displays the peak current of 6 μM BPA in PBS (0.1 M, pH 7) at various modified electrodes: SNGCE, AuNP(4 μl)/SNGCE, CB(0.5 μl)/AuNP(4)/SNGCE CB(1 μl)/AuNP(4 μl)/SNGCE, CB(2 μl)/AuNP(4 μl)/SNGCE and CB(2 μl)/SNGCE. At the bare SNGCE, the peak current of BPA was the lowest one and the peak potential was one of the more shifted towards more positive potential values (E = 0.47 V). Then, after the modification of the working electrode with AuSNPs, an increase of 100% of the peak current is obtained, along with a clear displacement of the peak towards more negative potential values (E = 0.43 V). Besides, the modification of the bare electrode with 2 μl of the CB dispersion increases the peak current around 5%, shifting much more the potential value towards more negative values (E = 0.33 V) with respect to the bare electrode. Furthermore, to evaluate the effect of CB amounts combined with a fixed volume of AuSNPs, the response of CB(0.5)/AuSNPs(4)/SNGCE, CB(1)/AuSNPs(4)/SNGCE and CB(2)/AuSNPs(4)/SNGCE for BPA detection was studied. As showed in Fig. 4, the presence of CB(2)/AuSNPs led to an increase of 690% of the peak intensity of the bare electrode compared with CB(0.5)/AuSNPs (E = 0.44 V) and CB(1)/AuSNPs (E = 0.50 V), which increased 30% and 54% the signal, respectively. Thus, as expected, the higher the CB volume drop-casted, the higher the peak intensity, causing this enormous improvement that can be attributed to the big active surface area, also the high conductivity of CB. As depicted in Fig. 4, a much higher oxidation peak for BPA detection 0.46 V was obtained using CB(2)/AuSNPs(4)/SNGCE compared with other oxidation peaks. Due to the enhanced electrocatalytic effect in the form of a clear increment in the peak current and a slight negative shifting of the peak potential caused by the combination of CB and AuSNPs, the CB(2)/AuSNPs(4)/SNGCE was used for further experiments.

### 3.2.2. pH effect

The pH influences on both, the reaction and BPA detection; for this reason, the effect of pH on the CB(2)/AuSNPs(4)/SNGCE sensor response for BPA detection was studied by DPV with the presence of 6 μM BPA in PBS (0.1 M) in the pH range 5.0–9.0 (Fig. 5). As displayed in Fig. 5.(a), the peak current of BPA increases with pH from pH 5.0 up to pH 7.0, then decreases. So, to improve the sensitivity, pH 7.0 value was selected in this work. A linear relationship was got between pH and the peak potential (E), reported by the following equation E = −0.051 pH + 0.834 (Fig. 5.(b)). The slope value obtained was 51 mV per pH unit, which is close to the theoretical value of 59 mV, showing that the electrons and protons number is equal.

### 3.2.3. Scan rate effect

The scan rate ($v$) effect on the peak current of BPA was also studied. Fig.6.(a) illustrates the influence of the scan rate at a CB(2)/AuSNPs(4)/SNGCE with the presence of 10 μM BPA in PBS (0.1 M, pH 7.0) by using cyclic voltammetry and ranging the scan rate in the interval 10–150 $mV{\cdot}s^{-1}$. As displayed in Fig.6.(b), the current peak, $I$, linearly increases with the values of scan rate, showing that the electrochemical detection of BPA at CB(2)/AuSNPs(4)/SNGCE is an adsorption-

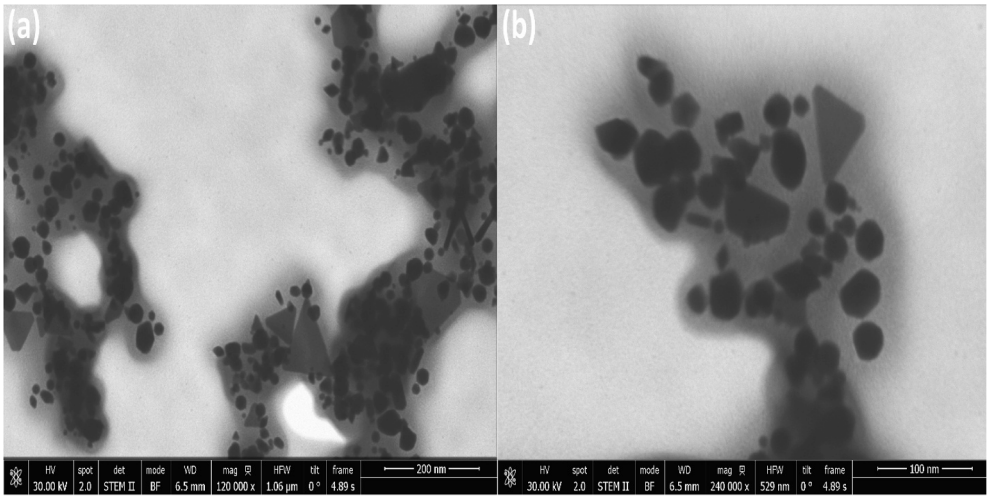


**Fig. 3.** STEM micrographs corresponding to AuSNPs synthesized with olive leaves extract at different magnifications: (a) 120,000× and (b) 240,000×.

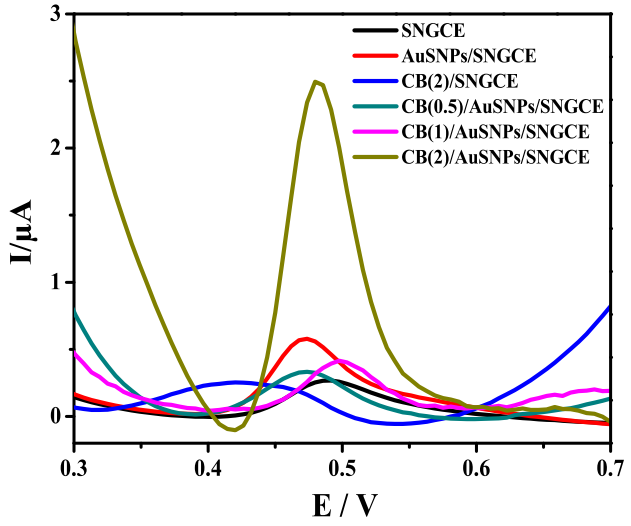


**Fig. 4.** DPV voltammograms corresponding to 6 μM BPA in PBS (0.1 M, pH 7.0) obtained with a scan rate of 60 $mV{\cdot}s^{-1}$ at different electrodes: SNGCE, AuSNPs (4)/SNGCE, CB(2)/SNGCE, CB(0.5)/AuSNPs(4)/SNGCE, CB(1)/AuSNPs(4)/SNGCE and CB(2)/AuSNPs(4)/SNGCE.

controlled process. Fig.6.(c) shown the variation of the peak potential (E) and the napierian logarithm of the scan rate (ln *v*). As it can be seen, the value of E shifted positively with the scan rate, due to the electrochemical reaction announced: $E = 0.033 \ln v + 0.497$ ($R^2 = 0.993$). As it is well known, the relationship between *E* and *ln v* for an adsorption-controlled process follows Laviron equation:

$$E = E^0 + (\alpha nF/RT)\ ln\ \left(RTK^0/\alpha nF\right) + (RT/\alpha nF)\ ln\ v$$

where $E^0$: is the redox potential, $K^0$: is the standard rate constant, n: is the number of the transferred electrons, R: is the gases universal constant, T: is the absolute temperature, and F: is the Faraday constant. The *αn* value can be obtained from the slope of E versus ln *v*. Here, the obtained slope is 0.033; thus, the calculated value of αn is 0.77. However, in an irreversible process, α is known to be 0.5. So, the calculated number n is around 2 (since $F = 96{,}485 C\ mol^{-1}$, $R = 8.314\ J\ K^{-1}\ mol^{-1}$, and $T = 298$ K). Thus, the mechanism for the oxidation reaction of BPA on the working electrode implicates two electrons and two protons, as depicted in Scheme 3.

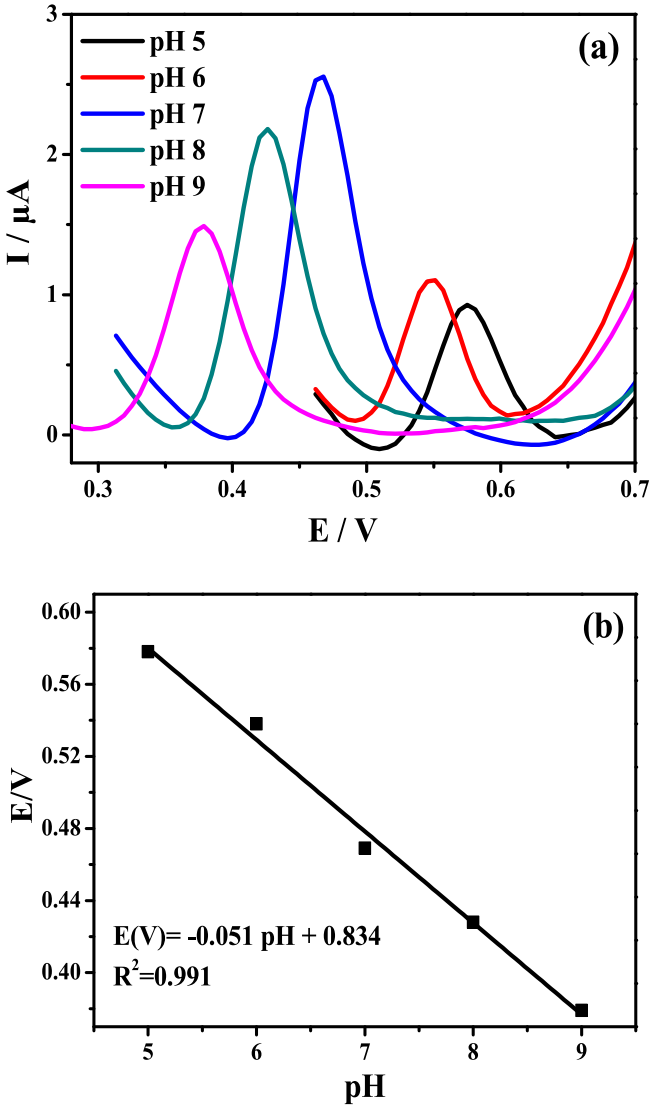


**Fig. 5.** Dependence of (a) peak current and (b) peak potential with respect to the pH value (5, 6, 7, 8 and 9). DPV voltammograms corresponds to 6 μM BPA at a CB(2)/AuSNPs(4)/SNGCE in PBS (0.1 M).

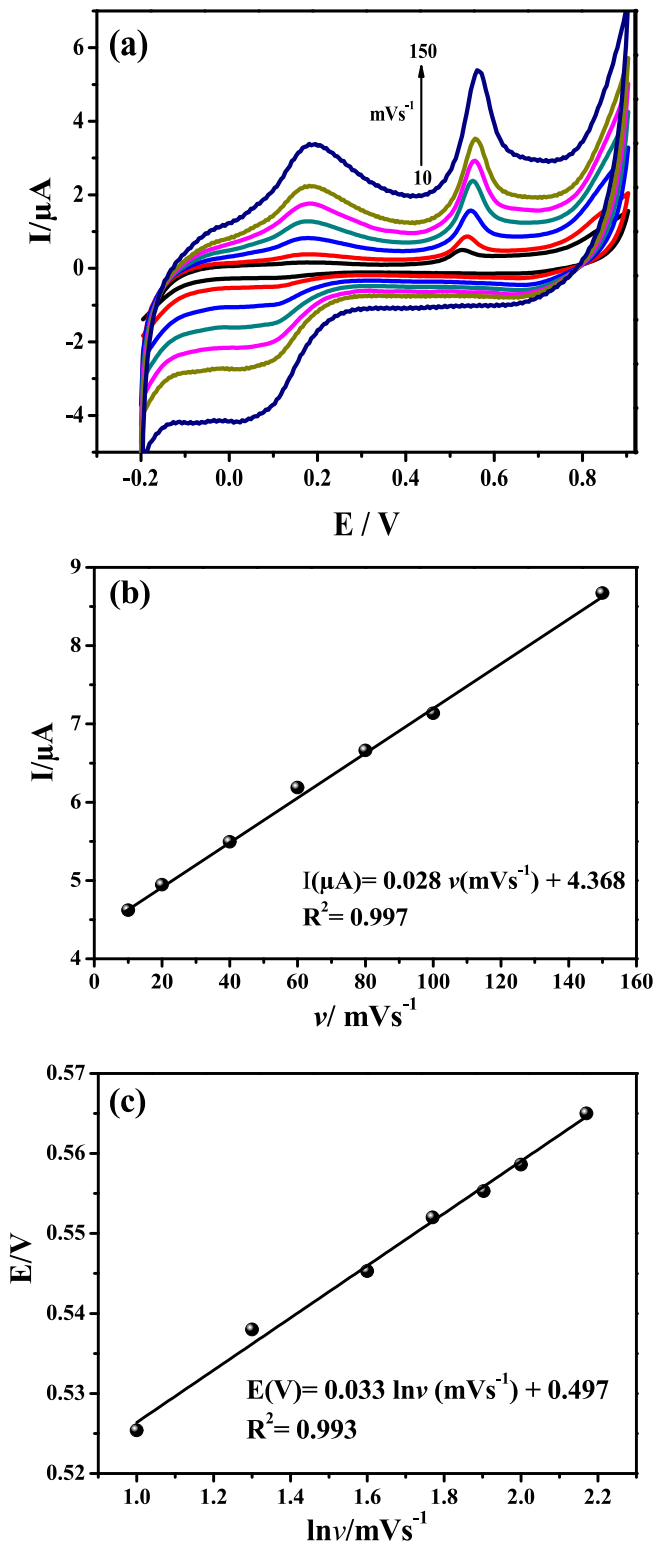


**Fig. 6.** (a) CV voltammograms obtained with a CB(2)/AuSNPs(4)/SNGCE of 10 µM BPA in PBS (0.1 M, pH 7.0) at various scan rates: 10, 20, 40, 60, 80, 100 and 150 mV $s^{-1}$; (b) plot of oxidation peak current, *I*, vs. $\nu$, and (c) the linear relationship between *E* and ln $\nu$.

### 3.2.4. Sensitivity study of the CB(2)/AuSNPs(4)/SNGCE

Under the optimized experimental parameters, our sensor was examined to evaluate its analytical performance. The CB(2)/AuSNPs(4)/SNGCE sensor was tested for the electrochemical determination of BPA at different concentrations with the range of 0.5–15 µM in PBS (0.1 M, pH 7.0) at 60 $mVs^{-1}$, observing the increase of the intensity current with increasing BPA concentrations. The calibration curve is shown in Fig. 7. (b) and follows the fitting equation: I(µA) = 0.342 [BPA](µM) + 0.122 ($R^2$ = 0.966). The sensitivity value is 0.342 A/M demonstrated the higher sensitivity of this proposed sensor. The limit of detection obtained according to the following equation: $(3 \times SD_{blank})/slope$ was 60 nM (n = 3). As shown in Table 1, the obtained LOD is one of the lowest reported in the literature. Furthermore, our developed sensor is the only one able to determine the BPA at nM level with the synergic combination of green AuSNPs and CB as cost-effective nanomaterials.

### 3.2.5. Reproducibility, repeatability and interference studies

The reproducibility was studied by testing the response of 10 µM of BPA with DPV, using three different electrodes, which were prepared similarly, showing a RSD of 1.61% (n = 3). The repeatability was examined by registering the response of 10 µM of BPA at three times successively employing the same working electrode, giving a RSD of 5.70% (n = 3). These results confirm that our developed sensor has excellent reproducibility and good repeatability.

The selectivity towards 1 µM of BPA was studied with the attendance of some interfering species at 100-fold high concentrations than the BPA concentrations, as illustrated in Table 2. The examined interferents species included: $Ca^{2+}$, $Mg^{2+}$, $Cu^{2+}$, phenol and hydroquinone. As shown in Table 2, none of the studied interferences displayed an important impact on the BPA response. The BPA peak varied just <10% both for inorganic and organic species. So, it could be concluded that our sensor could show good selectivity for BPA determination.

### 3.2.6. Surface and textural characterization of the modified SNGCE

Surface and textural characterization of the modified SNGCE with AuSNPs and CB/AuSNPs nanocomposite was carried out by SEM analysis. Fig. 8 illustrates the micrographs corresponding to two electrodes modified with AuSNPs. One of the electrodes has not been used in any electrochemical measurement, while the other electrode has been used at least 60 times for the electrochemical determination of BPA.

As shown in Fig. 8.(a) and (b), the SNGC material can be observed inside the glass capillary tubes. The presence of AuSNPs on the surface of SNGCE has been confirmed with the SEM images of backscattered electrons. Fig. 8.(c) showed small white dots on the electrode surface in large quantities, corresponding to the AuSNPs. Then, in the micrographs of the used electrode (Fig. 8.(b)), we can see that the amount of AuSNPs has decreased. Nevertheless, Fig. 8.(d) displayed that a large number of AuSNP clusters are still present on the surface of the electrode after 60 electrochemical measurements.

Fig. 9 shows the surface morphology of the CB/AuSNPs nanocomposite, evidencing that the nanostructures are very well dispersed on the working electrode surface (Fig. 9.(a)). The SEM images of used SNGCE modified with CB/AuSNPs nanocomposite after 60 electrochemical measurements are showed in Fig. 9.(b). It shows how the presence of nanocomposite on the surface of the electrode has decreased considerably. Also, we can see that there are gaps and cracks on the surface of the electrode, maybe due to the erosion that occurred through the utilize of the working electrode. Hence, despite any loss of nanocomposite from the electrode surface after successive measurements, the excellent performance of the developed eco-friendly sensor is not negatively affected.

### 3.2.7. Water samples applications

In order to estimate the performance of the CB(2)/AuSNPs(4)/SNGCE sensor in practical applications, the presence of BPA was tested in tap and mineral water samples. For this purpose, 5 ml PBS (pH 7.0, 0.1 M) was added to 5 ml of the corresponding sample; then the determination was accomplished using the previously optimized experimental parameters. Firstly, no BPA was found in the water sample; then, 2.5 and 15 µM of BPA concentrations were added to the sample and studied. The obtained results (see Table 3) showed that the recovery was

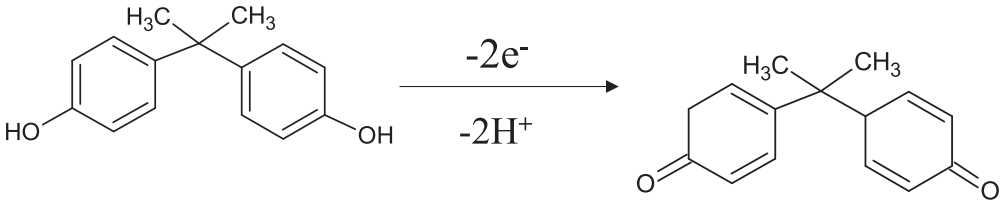


**Scheme 3.** Proposed mechanism for the oxidation reaction of BPA.

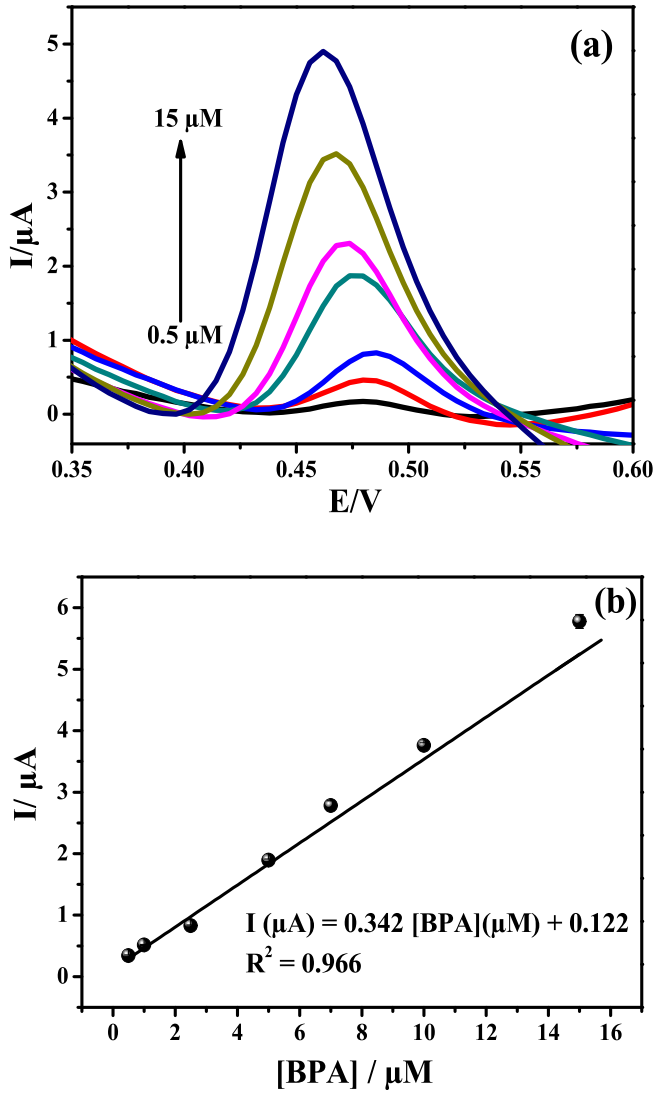


**Fig. 7.** (a) DPV voltammogram recorded at CB(2)/AuSNPs(4 µL)/SNGCE for increasing BPA concentrations (0.5, 1, 2.5, 5, 7, 10 and15 µM) in PBS (0.1 M, pH 7.0); (b) corresponding calibration plot.

in the range of 95.08% and 102.05%, with errors lower than 6%. These results indicate that our proposed sensor is suitable for real applications in water samples.

## 4. Conclusions

In this work, we propose a highly sensitive, selective, cost-effective, and environmentally friendly sensor for water monitoring of bisphenol A. The sensor is based on the Sonogel-Carbon electrode modified with a nanocomposite composed of novel and green AuSNPs, synthesized using olive leaves extract by a high energy ultrasound probe, and carbon black. The electrochemical performance of the BPA sensor was monitored by differential pulse voltammetry. The nanocomposite has an excellent catalytic activity for BPA determination thanks to the high surface area of the CB/AuSNPs nanocomposite. Different configurations for this sensor were tested, being the CB/AuSNPs/SNGCE sensor the one that shows clear analytical advantages: low limit of detection, high sensitivity and good stability and selectivity in the presence of 100-folds high interfering species concentration values. Moreover, the performance of the sensor is not negatively affected by successive and continuous use of the device. The proposed green sensor has been successfully applied in water real samples without any preliminary treatments. Thus, the CB/AuSNPs/SNGCE sensor achieved desirable BPA sensing capabilities, being a very promising sensor for sustainable applications such as the monitoring of water security.

**Table 1**
Comparison of our proposed sensor with other published sensors for the determination of BPA.

| Electrode material | Electroanalytical technique | Linear range/µM | Limit of detection/µM | Ref. |
|---|---|---|---|---|
| MIPs/MNPs/CTAB/CPE | CV | 0.6–100 | 0.10 | [40] |
| $NH_2$-MIL-125/RGO/GCE | DPV | 2–200 | 0.79 | [41] |
| Thionine–CB/SPE | CV | 0.5–50 | 0.20 | [42] |
| MIP–AuNPs/GCE | Amperometry | 8–6 × $10^4$ | 0.138 | [43] |
| PEDOT/GCE | CV | 90–410 | 55 | [44] |
| | Amperometry | 40–410 | 22 | |
| EG | SWV | 1.56–50 | 0.76 | [45] |
| CAS-CB/GCE | LS | 0.49–24 | 0.25 | [46] |
| AgNPs/GPUE | DPV | 2.5–15 | 0.24 | [47] |
| CPE | DPV | 0.5–6 | 0.36 | [48] |
| CBPE | DPV | 0.5–4 | 0.80 | |
| CNTPE | DPV | 1–4 | 0.70 | |
| CB/AuSNPs/SNGCE | DPV | 0.5–15 | 0.06 | This work |

MIPs: molecularly imprinted polymers; MNPs: magnetic nanoparticles; CTAB: cetyltrimethyl ammonium bromide; CPE: carbon paste electrode; $NH_2$-MIL-125/RGO: amine-functionalized metal-organic framework/reduced graphene oxide; GCE: glassy carbon electrode; SPE: Screen printed electrode; PEDOT: poly(3,4-ethylenedioxythiophene); EG: exfoliated graphite; CAS: casein; LS: linear scan. SWV: square wave voltammetry technique; AgNPs: silver nanoparticles; GPUE: graphite-polyurethane composite electrodes; CBPE: carbon paste electrode based on carbon black; CNTPE: carbon paste electrode based on carbon nanotubes.

**Table 2**
Interferents effect, with 100 µM concentration, on the response towards 1 µM BPA.

| Interferents | Peak change (%) |
|---|---|
| $Ca^{2+}$ | 2.15 |
| $Mg^{2+}$ | −3.27 |
| $Cu^{2+}$ | 5.57 |
| Phenol | 9.33 |
| Hydroquinone | −6.80 |

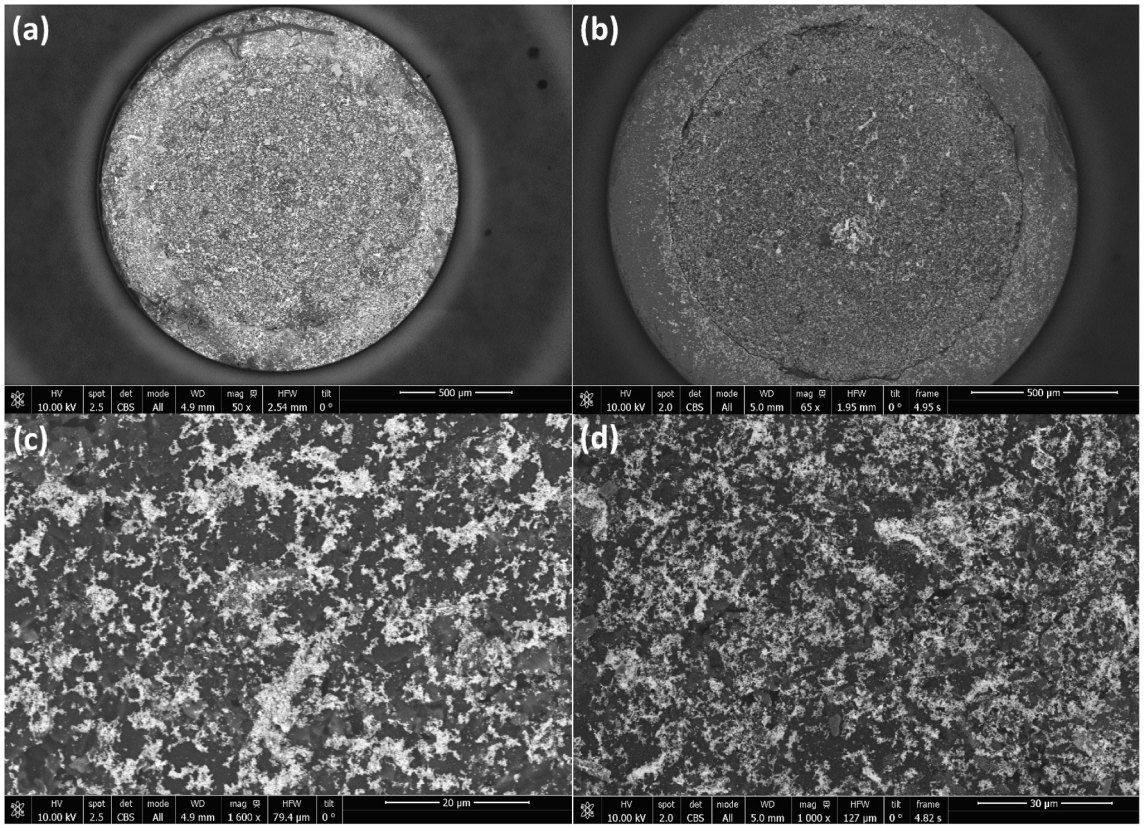


**Fig. 8.** SEM micrographs corresponding to AuSNPs-modified electrodes: (a), (c) not used and (b), (d) used.

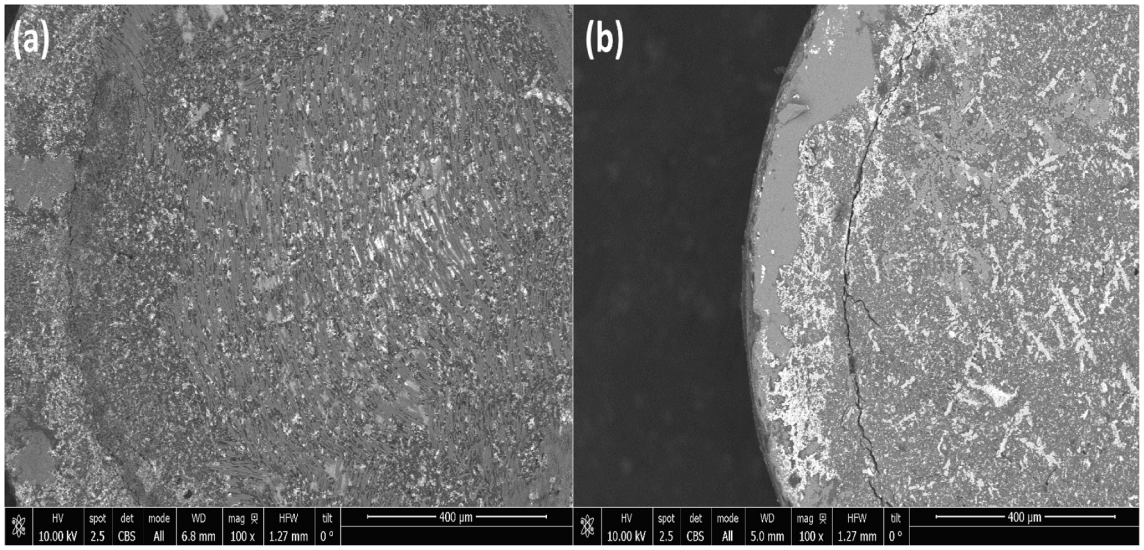


**Fig. 9.** SEM micrographs corresponding to CB/AuSNPs nanocomposite-modified electrodes: (a) not used and (b) used.

**Table 3**
Recovery percentages and errors obtained after electrochemical detection of BPA in tap and mineral water samples.

| Samples | Added (μM) | Found (μM) | Recovery (%) | RSD[a] (%) |
|---|---|---|---|---|
| Mineral water | 2.5 | 2.34 | 102.05 | 2.01 |
| | 15 | 14.76 | 96.49 | 3.63 |
| Tap water | 2.5 | 2.39 | 101.56 | 1.54 |
| | 15 | 14.96 | 95.08 | 5.16 |

[a] n = 3.

## Declaration of Competing Interest

The authors declare that they have no known competing financial interests or personal relationships that could have appeared to influence the work reported in this paper.

## Acknowledgments

Siwar Jebril gratefully acknowledges financial support from Erasmus+ KA107 Program of the University of Cadiz (Spain), through

Servicio Español para la Internacionalización de la Educación (SEPIE) funds from EU. Authors would like to thank the Tunisian MHESR for supporting this work and the University of Sousse for the "Bourse d'alternance" fellowship awarded to Siwar Jebril. Authors also greatly acknowledge Junta de Andalucía and Institute of Research on Electron Microscopy and Materials (IMEYMAT – BIOSENSEP project) for their financial support, and Banco de Santander (Spain), Aula del Estrecho and Oficina de Relaciones Internacionales of University of Cadiz for the support given through the international collaboration project: 003ENE2019: 'Fortalecimiento de la colaboración en materia de investigación en el área de química con la Universidad de Sousse: síntesis ecológica y caracterización de nanoestructuras metálicas. Aplicación en agricultura y medioambiente', (Call 2018/2019 – Resolución del Rector de la Universidad de Cádiz UCA/R96REC/2018 de 31 de octubre de 2018). Finally, authors thank 'Programa de fomento e impulso de la investigación y de la transferencia de la Universidad de Cádiz 2018-2019' for the funds given through the project PR2018-070 (Proyectos de Investigación-Puente 2018).

## References

[1] N.B. Messaoud, A.A. Lahcen, C. Dridi, A. Amine, Ultrasound assisted magnetic imprinted polymer combined sensor based on carbon black and gold nanoparticles for selective and sensitive electrochemical detection of bisphenol A, Sensors Actuators B Chem. 276 (2018) 304–312.
[2] D. Jemmeli, E. Marcoccio, D. Moscone, C. Dridi, F. Arduini, Highly sensitive paper-based electrochemical sensor for a reagent free detection of bisphenol A, Talanta 216 (2020) 120924–120931.
[3] N.B. Messaoud, M.E. Ghica, C. Dridi, M.B. Ali, C.M. Brett, Electrochemical sensor based on multiwalled carbon nanotube and gold nanoparticle modified electrode for the sensitive detection of bisphenol A, Sensors Actuators B Chem. 253 (2017) 513–522.
[4] A. Schecter, N. Malik, D. Haffner, S. Smith, T.R. Harris, O. Paepke, L. Birnbaum, Bisphenol A (BPA) in US food, Environ. Sci. Technol. 44 (2010) 9425–9430.
[5] J. Im, F.E. Löffler, Fate of bisphenol A in terrestrial and aquatic environments, Environ. Sci. Technol. 50 (2016) 8403–8416.
[6] Z. Liu, Y. Li, L. Sun, H. Yang, X. Zheng, L. Wang, Investigation of diazo-derivatization of bisphenol A and its applicability for quantitation in food safety inspections using high-performance liquid chromatography, Biomed. Chromatogr. 33 (2019) e4419.
[7] D. Tan, J. Jin, L. Wang, X. He, C. Guo, X. Lu, J. Chen, Quantification of bisphenol A and its selected analogs in serum using pre-column derivatization with high-performance liquid chromatography and tandem mass spectrometry, J. Sep. Sci. 42 (2019) 991–998.
[8] X. Zhang, D. Zhu, C. Huang, Y. Sun, Y.-I. Lee, Sensitive detection of bisphenol A in complex samples by in-column molecularly imprinted solid-phase extraction coupled with capillary electrophoresis, Microchem. J. 121 (2015) 1–5.
[9] S.M. Jung, H.-J. Kim, B.-J. Kim, G.-S. Joo, T.-S. Yoon, Y.-S. Kim, H.H. Lee, Amperometric detection of bisphenol-A on laser fabricated capillary electrophoresis device, Biochip Journal 3 (2009) 219–223.
[10] H. Ohkuma, K. Abe, M. Ito, A. Kokado, A. Kambegawa, M. Maeda, Development of a highly sensitive enzyme-linked immunosorbent assay for bisphenol A in serum, Analyst. 127 (2002) 93–97.
[11] G.R. Marchesini, E. Meulenberg, W. Haasnoot, H. Irth, Biosensor immunoassays for the detection of bisphenol A, Anal. Chim. Acta 528 (2005) 37–45.
[12] E. Jo, J. Lee, Polyaniline-nanofiber-modified screen-printed electrode with intermediate dye amplification for detection of endocrine disruptor bisphenol A, Microchem. J. 155 (2020) 104693.
[13] Y. Wang, C. Yin, Q. Zhuang, An electrochemical sensor modified with nickel nanoparticle/nitrogen-doped carbon nanosheet nanocomposite for bisphenol A detection, J. Alloys Compd. 827 (2020) 154335.
[14] F. Arduini, F. Di Nardo, A. Amine, L. Micheli, G. Palleschi, D. Moscone, Carbon black-modified screen-printed electrodes as electroanalytical tools, Electroanalysis. 24 (2012) 743–751.
[15] X. Zhang, Y. Cui, Z. Lv, M. Li, S. Ma, Z. Cui, Q. Kong, Carbon nanotubes, conductive carbon black and graphite powder based paste electrodes, Int. J. Electrochem. Sci. 6 (2011) 6063–6073.
[16] F.C. Vicentini, A.E. Ravanini, L.C. Figueiredo-Filho, J. Iniesta, C.E. Banks, O. Fatibello-Filho, Imparting improvements in electrochemical sensors: evaluation of different carbon blacks that give rise to significant improvement in the performance of electroanalytical sensing platforms, Electrochim. Acta 157 (2015) 125–133.
[17] F. Arduini, C. Zanardi, S. Cinti, F. Terzi, D. Moscone, G. Palleschi, R. Seeber, Effective electrochemical sensor based on screen-printed electrodes modified with a carbon black-Au nanoparticles composite, Sensors Actuators B Chem. 212 (2015) 536–543.
[18] I. Razavipanah, G.H. Rounaghi, B. Deiminiat, S. Damirchi, K. Abnous, M. Izadyar, M. Khavani, A new electrochemical aptasensor based on MWCNT-SiO2@Au core-shell nanocomposite for ultrasensitive detection of bisphenol A, Microchem. J. 146 (2019) 1054–1063.
[19] J. Cai, B. Sun, W. Li, X. Gou, Y. Gou, D. Li, F. Hu, Novel nanomaterial of porous graphene functionalized black phosphorus as electrochemical sensor platform for bisphenol A detection, J. Electroanal. Chem. 835 (2019) 1–9.
[20] A. Thamilselvan, V. Rajagopal, V. Suryanarayanan, Highly sensitive and selective amperometric determination of BPA on carbon black/f-MWCNT composite modified GCE, J. Alloys Compd. 786 (2019) 698–706.
[21] U.H. Bunz, V.M. Rotello, Gold nanoparticle–fluorophore complexes: sensitive and discerning "noses" for biosystems sensing, Angew. Chem. Int. Ed. 49 (2010) 3268–3279.
[22] J. Du, H. Singh, W. Dong, Y. Bai, T.-H. Yi, Colorimetric detection of Listeria monocytogenes using one-pot biosynthesized flower-shaped gold nanoparticles, Sensors Actuators B Chem. 265 (2018) 285–292.
[23] N.M.Y. Zhang, M. Qi, Z. Wang, Z. Wang, M. Chen, K. Li, P. Shum, L. Wei, One-step synthesis of cyclodextrin-capped gold nanoparticles for ultra-sensitive and highly-integrated plasmonic biosensors, Sensors Actuators B Chem. 286 (2019) 429–436.
[24] K.-J. Huang, Y.-J. Liu, Y.-M. Liu, L.-L. Wang, Molybdenum disulfide nanoflower-chitosan-Au nanoparticles composites based electrochemical sensing platform for bisphenol A determination, J. Hazard. Mater. 276 (2014) 207–215.
[25] H. Yin, Y. Zhou, S. Ai, R. Han, T. Tang, L. Zhu, Electrochemical behavior of bisphenol A at glassy carbon electrode modified with gold nanoparticles, silk fibroin, and PAMAM dendrimers, Microchim. Acta 170 (2010) 99–105.
[26] T. Dayakar, K.V. Rao, K. Bikshalu, V. Rajendar, S.-H. Park, Novel synthesis and structural analysis of zinc oxide nanoparticles for the non enzymatic glucose biosensor, Mater. Sci. Eng. C 75 (2017) 1472–1479.
[27] S. Jebril, R. Khanfir Ben, C. Dridi Jenana, Green synthesis of silver nanoparticles using *Melia azedarach* leaf extract and their antifungal activities: in vitro and in vivo, Mater. Chem. Phys. 248 (2020) (122898).
[28] H. Chandra, P. Kumari, E. Bontempi, S. Yadav, Medicinal plants: treasure trove for green synthesis of metallic nanoparticles and their biomedical applications, Biocatalysis and Agricultural Biotechnology 24 (2020), 101518.
[29] A. Singh, P.K. Gautam, A. Verma, V. Singh, P.M. Shivapriya, S. Shivalkar, A. K. Sahoo, S.K. Samanta, Green synthesis of metallic nanoparticles as effective alternatives to treat antibiotics resistant bacterial infections: a review, Biotechnology Reports 25 (2020) e00427.
[30] M. Franco-Romano, M.L.A. Gil, J.M. Palacios-Santander, J.J. Delgado-Jaén, I. Naranjo-Rodríguez, J.L. Hidalgo-Hidalgo de Cisneros, L.M. Cubillana-Aguilera, Sonosynthesis of gold nanoparticles from a geranium leaf extract, Ultrason. Sonochem. 21 (2014) 1570–1577.
[31] M.M. Cordero-Rando, J.L. Hidalgo-Hidalgo de Cisneros, E. Blanco, I. Naranjo-Rodríguez, The sonogel-carbon electrode as a sol-gel graphite-based electrode, Anal. Chem. 74 (2002) 2423–2427.
[32] L.M. Cubillana-Aguilera, J.M. Palacios-Santander, I. Naranjo-Rodríguez, J. L. Hidalgo-Hidalgo-de-Cisneros, Study of the influence of the graphite powder particle size on the structure of the sonogel-carbon materials, J. Sol-Gel Sci. Technol. 40 (2006) 55–64.
[33] Y. Guo, N. Jiang, L. Zhang, M. Yin, Green synthesis of gold nanoparticles from Fritillaria cirrhosa and its anti-diabetic activity on Streptozotocin induced rats, Arab. J. Chem. 13 (2020) 5096–5106.
[34] A.I. Usman, A.A. Aziz, O.A. Noqta, Green sonochemical synthesis of gold nanoparticles using palm oil leaves extracts, Materials Today: Proceedings 7 (2019) 803–807.
[35] M.M.H. Khalil, E.H. Ismail, F. El-Magdoub, Biosynthesis of Au nanoparticles using olive leaf extract, Arab. J. Chem. 5 (2012) 431–437.
[36] N. Thangamani, N. Bhuvaneshwari, Green synthesis of gold nanoparticles using Simarouba glauca leaf extract and their biological activity of micro-organism, Chem. Phys. Lett. 732 (2019) 136587.
[37] T. Song, F. Gao, Y. Zhang, C. Wang, Y. Shiraishi, S. Li, C. Wang, J. Guo, Y. Du, Shape-controlled PdSn alloy as superior electrocatalysts for alcohol oxidation reactions, J. Taiwan Inst. Chem. Eng. 101 (2019) 167–176.
[38] Z. Cai, Y. Ye, X. Wan, J. Liu, S. Yang, Y. Xia, G. Li, Q. He, Morphology–dependent electrochemical sensing properties of iron oxide–graphene oxide nanohybrids for dopamine and uric acid, Nanomaterials. 9 (2019) 835.
[39] S.G. Jiji, K.G. Gopchandran, Shape dependent catalytic activity of unsupported gold nanostructures for the fast reduction of 4-nitroaniline, Colloid and Interface Science Communications 29 (2019) 9–16.
[40] L. Zhu, Y. Cao, G. Cao, Electrochemical sensor based on magnetic molecularly imprinted nanoparticles at surfactant modified magnetic electrode for determination of bisphenol A, Biosens. Bioelectron. 54 (2014) 258–261.
[41] L.J. Ling, J.P. Xu, Y.H. Deng, Q. Peng, J.H. Chen, Y. San He, Y.J. Nie, One-pot hydrothermal synthesis of amine-functionalized metal–organic framework/reduced graphene oxide composites for the electrochemical detection of bisphenol A, Anal. Methods 10 (2018) 2722–2730.
[42] M. Portaccio, D. Di Tuoro, F. Arduini, D. Moscone, M. Cammarota, D.G. Mita, M. Lepore, Laccase biosensor based on screen-printed electrode modified with thionine–carbon black nanocomposite, for bisphenol A detection, Electrochim. Acta 109 (2013) 340–347.
[43] J. Huang, X. Zhang, S. Liu, Q. Lin, X. He, X. Xing, W. Lian, Electrochemical sensor for bisphenol A detection based on molecularly imprinted polymers and gold nanoparticles, J. Appl. Electrochem. 41 (2011) 1323.
[44] E. Mazzotta, C. Malitesta, E. Margapoti, Direct electrochemical detection of bisphenol A at PEDOT-modified glassy carbon electrodes, Anal. Bioanal. Chem. 405 (2013) 3587–3592.
[45] T. Ndlovu, O.A. Arotiba, S. Sampath, R.W. Krause, B.B. Mamba, An exfoliated graphite-based bisphenol A electrochemical sensor, Sensors. 12 (2012) 11601–11611.

[46] L. Vieira Jodar, L.O. Orzari, T. Storti Ortolani, M.H. Assumpção, F.C. Vicentini, B. C. Janegitz, Electrochemical sensor based on casein and carbon black for bisphenol A detection, Electroanalysis. 31 (2019) 2162–2170.
[47] M. Baccarin, M. Ciciliati, O.N. Oliveira, E.T.G. Cavalheiro, P.A. Raymundo-Pereira, Pen sensor made with silver nanoparticles decorating graphite-polyurethane electrodes to detect bisphenol-A in tap and river water samples, Mater. Sci. Eng. C 110989 (2020).
[48] A. Ghanam, A.A. Lahcen, A. Amine, Electroanalytical determination of bisphenol A: investigation of electrode surface fouling using various carbon materials, J. Electroanal. Chem. 789 (2017) 58–66.